[논문] 한국태양에너지학회 논문집
Journal of the Korean Solar Energy Society

Vol. 35, No. 4, 2015
ISSN 1598-6411
http://dx.doi.org/10.7836/kses.2015.35.4.043

V 형 rib과 dimple로 구성된 SAH 덕트에서의 총괄 열성능에 대한 수치적 연구

Numerical study on overall thermal performance in SAH duct with compound roughness of V-shaped ribs and dimples

아닐 쿠마르* · 김만회**†
Anil Kumar* and Man-Hoe Kim**†

(Received 13 July 2015; Accepted 25 August 2015)

Abstract : This paper presents the thermal hydraulic performance of a three dimensional rib-roughened solar air heater (SAH) duct with the one principal wall subjected to uniform heat flux. The SAH duct has aspect ratio of 12.0 and the Reynolds number ranges from 2000 to 12000. The roughness has relative rib height of 0.045, ratio of dimple depth to print diameter of 0.5 and rib pitch ratio of 8.0. The flow attack angle is varied from 35° to 70°. Various turbulent flow models are used for the heat transfer and fluid flow analysis and their results are compared with the experimental results for smooth surfaces. The computational fluid dynamics (CFD) results based on the renormalization k-epsilon model are in better outcomes compared with the experimental data. This model is used to calculate heat transfer and fluid flow in SAH duct with the compound roughness of V-shaped ribs and dimples. The overall thermal performance based on equal pumping power is found to be the highest (2.18) for flow attack angle of 55°. The thermo-hydraulic performance for V-pattern shaped ribs combined with dimple ribs is higher than that for dimple rib shape and V-pattern rib shape air duct.

Key Words : 전산유체역학(CFD, Computational fluid dynamics), 태양가열기(SAH, Solar air heater), 유동입사각(Flow attack angle), 전열촉진(Heat transfer enhancement), 총괄 열성능(Overall thermal performance), V-형 rib과 dimple 로 구성된 표면(Roughness of V-shaped ribs and dimples)

**† 김만회(교신저자) : 경북대학교 기계공학부
E-mail : manhoe.kim@knu.ac.kr, Tel : 053-950-5576
* 아닐 쿠마르 : 경북대학교 기계공학부

**† Kim Man-Hoe(corresponding author) : School of Mechanical Engineering, Kyungpook National University.
E-mail : manhoe.kim@knu.ac.kr, Tel : 053-950-5576
* Anil Kumar : School of Mechanical Engineering, Kyungpook National University

Nomenclature

D : Hydraulic diameter of air duct (m)
e : Rib height (m)
e/D : relative roughness height
E : Total energy (J)
f : Friction factor
H : Depth of SAH duct (m)
L : Length of test section (m)
Nu : Nusselt number
P : Rib pitch (m)
P/e : Relative roughness pitch
p : Pressure (Pa)
Pr : Prandtl number
Re : Reynold number
S : Modulus of strain tensor
s : Length of metal grit rib (m)
St : Stanton number
u : Velocity (m/s)
V : Velocity of air (m/s)
SAH : Solar air heater

Greek Symbols

ave : Average
i, j, k : Tensor for i, j, k direction
s : Smooth surface

Subscript

a : Flow attack angle (°)
β : Thermal expansion coefficient (1/K)
μ : Viscosity (Ns/m^2)
μ_t : Turbulent viscosity (Ns/m^2)
ρ : Density (kg/m^3)
η : Overall performance parameter
ε : Energy dissipation rate (m^2/s^3)

1. Introduction

Solar energy is a type of clean and freely available renewable energy that can be simply utilized for heating applications upon conversion into thermal energy by using solar air heaters (SAHs). Due to their simplicity, cheapness, and little maintenance requirements, SAHs are widely used for solar energy collection. However, Thermal efficiency of SAH is significantly low because of low convective heat transfer coefficient between the absorber plate and air, leading to high absorber plate temperature and greater amount of heat losses to the ambient. It has been found that the main thermal resistance to the convective heat transfer is due to the formation of boundary layer on the heat transferring surface.[1-3] Efforts for enhancing heat transfer have been directed towards artificially destroying or disturbing this boundary layer. Although the use of artificial roughness on the underside of the absorber plate can substantially enhance the thermal performance of the SAH due to increase in heat transfer coefficient, however, it is necessary that while creating turbulence to break the laminar sublayer, the core flow should not be disturbed so as to avoid excessive friction losses. This can be achieved by using artificial roughness with roughness height being such that it does not project

deep into the core but just projects out of laminar sublayer.[1-5)]

The rib roughened surface has wide application namely in cooling of gas turbine blades, nuclear reactors, solar air heating systems etc. The application of artificial roughness enhances the heat transfer at the cost of increased value of friction factor and power penalty. The efforts of the researchers are always directed towards the proper selection of the shape and arrangement of the artificial roughness, which modifies the boundary layer, enhances the heat transfer coefficient with minimum pressure drop i.e. power penalty.[3,4)] The concept of artificial roughness was first applied to enhance heat transfer coefficients for in-tube condensation of steam and since then many experimental investigations were carried out on the application of artificial roughness in the areas of cooling of gas turbine, electronic equipment's, nuclear reactors, and compact heat exchangers etc.[5,6)] Han et al.[7)] experimentally investigated the effects of rib shape, angle of attack and pitch-to-rib height ratio on friction factor and heat transfer coefficient. Park et al.[8)] presented the results of heat transfer and friction factor data measured in five short rectangular channels with turbulence promoters. Lau et al.[9)] carried out experiments to study the turbulent heat transfer and friction for fully developed flow of air in a square channel with discrete rib turbulators. Zhang et al.[10)] investigated the effect of compound turbulaors on friction factors and heat transfer coefficients in rectangular channels with two opposite ribbed-grooved walls. Prasad and Mullick[11)] were the first who introduced the application of artificial roughness in the form of small diameter wire attached on the underside of absorber plate to improve the thermal performance of SAH for drying purposes.

Other detailed descriptions of several experimental investigations on ribs with different shapes may be found from the references.[12-23)] Taslim et al.[20)] presented the effect of V-shaped rib roughness with variation of relative rib height, relative rib pitch and flow attack angle on heat transfer and friction factor in a flow through SAH duct. They reported that the V-shaped rib showed higher performance compared to the angled rib. For the range of Reynolds number and duct aspect ratio normally used in SAH, the V-shape rib pointing downstream results in higher heat transfer and friction factor than those pointing upstream. Momin et al.[22)] conducted an experimental study on heat transfer and pressure drop for the turbulent flow through a channel with one wall roughened by using an V-shaped rib. They varied the flow attack angle of the V-shaped rib roughness and examined its effect on the heat transfer and pressure drop in an SAH. They observed that V-shaped rib of an extended angled rib benefits in the formation of two secondary stream cells as compared to one in case of an angled rib resultant in still higher heat transfer rate. Saini and Verma[23)] reported the experimental results of the turbulent fluid flow and heat

transfer characteristics in a rectangular air channel with a dimpled roughness shape attached to the underside of a heated plate. They changed the range of Reynolds number from 2000 to 12000 with the relative roughness heights of 0.018-0.037 and the relative roughness pitches of 8-12. For the range of parameters investigated, Nusselt number was found to be the maximum corresponding to relative roughness height of 0.0379 and relative roughness pitch of 10. Computational Fluid Dynamics (CFD) is another approach to solve the problem of fluid flow and heat transfer in a rib roughness air duct. The benefits of CFD in relation to experiments are that it is much cheaper and less time consuming. A critical review of literatures on rib roughened air duct reveals that very few studies are used CFD.[6, 24-30]

To the best of our knowledge, no such type of CFD study has been reported on an artificially roughened air duct with V-shaped ribs combined with dimple ribs. The purpose of this work was to investigate fluid flow and heat transfer characteristics of a three-dimensional rectangular duct of an air duct with V with dimpled ribs by adopting the CFD approach. A commercial CFD software - ANSYS (Fluent 6.3.26) is used to predict the heat transfer and flow characteristics with V-shaped ribs combined with dimple ribs on the heated plate as artificial roughness. The main objectives of the numerical analysis were as follows: (1) Investigate the effect of flow attack angle on the average Nusselt number, average friction factor, and thermo-hydraulic performance parameters. (2) Determination of the optimal thermo-hydraulic performance parameter under the same pumping power constraint to examine the overall effect of the flow attack angle.

2. Numerical procedure

2.1 Problem description

The three-dimensional air duct model, depicted in Fig.1, has an L = 1000 mm while the H is set equal to 25 mm and W is 300 mm; the hydraulic diameter, $D = 4A/P = 2H$, is equal to 12.0 mm. The 3 mm thick wall is made up by aluminum and a constant heat flux of 1000 W/m^2 has been applied. The roughness parameters are determined by rib height(e), rib pitch(P), print diameter of dimple rib (d_d), angle of attack (a) and the shape of the roughness elements. For a specific roughness type, a family of geometrically similar roughness is possible to identify by changing flow angle attack while maintaining constant, P/e, e/D and e/d_d. The range of dimensionless roughness parameters employed in this investigation are given in Table.1.

Table 1 Range of parameters

Parameters	Range
Reynolds number, Re	2000 - 12000
Relative roughness pitch, P/e	8.0
Relative roughness height, e/D	0.045
Dimple depth/print diameter, e/d_d	0.5
Flow attack angle, a	35° - 75°

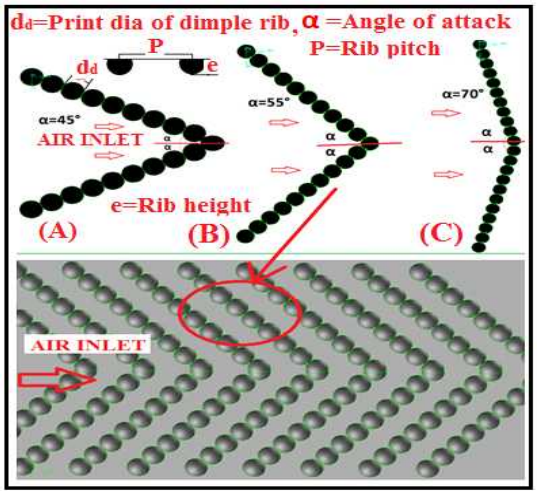

Fig. 1 Solution domain for CFD analysis

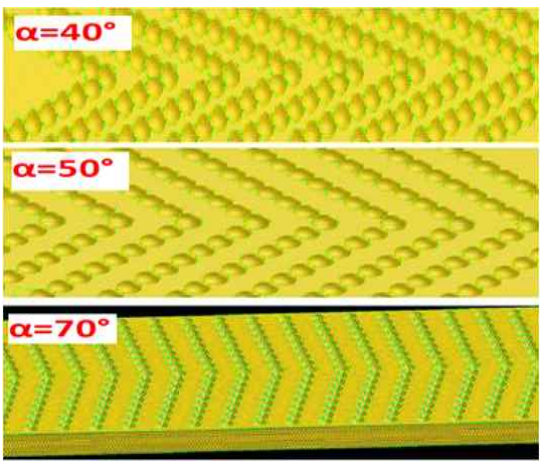

Fig. 2 Grid generation of different flow angle attacks

2.2 Grid generation

A grid independence check is essential in order to get reasonable results, which are independent of the number of grid cells. In the present case, a number of runs on different mesh density are made. To change the grid density the grid adaption for temperature gradient is used. If the results from the finest and the next finest mesh are nearly equal, the results are considered to be grid independent. The results given here are those obtained after satisfying the grid independence test. The above analyses are carried out using different selected turbulence models to find out variation of Nus_{ave} and fs_{ave} with Re for the range between 2000 and 12000 and compared with the experimental results. The different thermo physical of air properties like thermal conductivity, viscosity, specific heat, density involved are evaluated at working pressure and temperature of air in the duct. The different V-down shaped ribs combined with dimpled rib shapes caused secondary streams to occur. Hence, the possibility of using two-dimensional domains and grids was ruled out. Therefore, 3-D domains and meshes were selected, as shown in Fig.2. In order to accurately study the stream and heat transfer in the inter-rib regions, adequate meshing at these places was performed. In other sections, a coarser mesh was applied. In the current work, the grids were created using the ANSYS software.

2.3 Governing equations

Three dimensional CFD simulations of the heat transfer and flow friction appearances are conducted by using the ANSYS FLUENT. The simulation was carried out in order to calculate and explain the experimental conditions. The CFD simulation involves numerical solutions of the conservation equations for mass, momentum and energy. These equations for incompressible streams can be written as follows.[24-30]:

Continuity equation:

$$\frac{\partial}{\partial x_j}(\rho u_j) = 0 \tag{1}$$

Momentum equation:

$$\frac{\partial}{\partial x_j}(\rho u_i u_j) = -\frac{\partial p}{\partial x_j} + \frac{\partial}{\partial x_j}\left[\mu\left(\frac{\partial u_i}{\partial x_j} + \frac{\partial u_j}{\partial x_i}\right)\right] - (\rho\overline{u_i u_j}) \tag{2}$$

Energy equation:

$$\frac{\partial}{\partial x_j}(\rho u_j T) = \frac{\partial}{\partial x_j}\left[\left(\frac{\mu}{\mathrm{Pr}} + \frac{\mu_t}{\sigma_t}\right)\frac{\partial T}{\partial x_j}\right] \tag{3}$$

The Reynolds-averaged method of turbulence simulation requires suitable modeling of the Reynolds stresses, $(\rho\overline{u_i u_j})$ in Eq. (2). A common technique employs the Boussinesq approximation to relate the Reynolds strains to the average velocity gradients.

$$-(\rho\overline{u_i u_j}) = \mu_t\left(\frac{\partial u_i}{\partial x_j} + \frac{\partial u_j}{\partial x_i}\right) - \frac{2}{3}k\delta_{ij} \tag{4}$$

The turbulent viscosity term can be calculated from a suitable turbulence model. The appearance of the turbulent viscosity is specified as

$$\mu_t = \rho C_\mu \frac{k^2}{\epsilon} \tag{5}$$

The transport equations for k and ε are:

$$\frac{\partial}{\partial x_j}(\rho k u_j) = \frac{\partial}{\partial x_j}\left[\left(\mu + \frac{\mu_t}{\sigma_k}\right)\frac{\partial k}{\partial x_j}\right] + G_k - \sigma\epsilon \tag{6}$$

$$\frac{\partial}{\partial x_j}(\rho\epsilon u_j) = \frac{\partial}{\partial x_j}\left[\left(\mu + \frac{\mu_t}{\epsilon_k}\right)\frac{\partial \epsilon}{\partial x_j}\right] + C_{1\epsilon}\frac{\epsilon}{k}G_k - C_{2\epsilon}\rho\frac{\epsilon^2}{k} \tag{7}$$

where $G_k = -(\rho\overline{u_i u_j})\frac{\partial u_i}{\partial x_j}$ represents the production of turbulent kinetic energy. The boundary conditions for the V-shaped ribs combined with dimple ribs are applied as experimental conditions.[7-18]

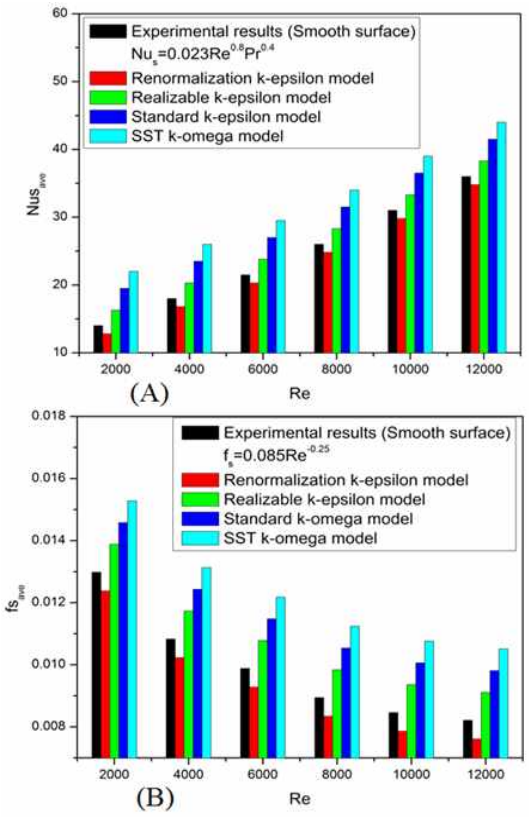

Fig. 3 Comparison CFD and experimental results

2.4 Validation of numerical model

For validation of turbulence models, the CFD results of Nus_{ave} and fs_{ave} were compared

with experimental data for smooth surface SAH duct. The following Dittus-Boelter and modified Blasius equations for Nu and f were used, respectively.

$$Nus_{ave} = 0.023 Re^{0.8} \mathrm{Pr}^{0.4} \quad (8)$$

$$fs_{ave} = 0.085 Re^{-0.25} \quad (9)$$

Fig.3 shows the CFD results of Nus_{ave} and fs_{ave} against Re for various models compared with experimental results for smooth surface. The results by using RNG k-ε model shows the best agreement with experimental results. It is therefore, RNG k-ε model has been employed for the present CFD study.

3. Results and discussion

3.1 Thermal counters

Fig.4 shows the velocity profiles for the V-down shaped ribs combined with dimple ribs with different values of a = 35°-70°, and kept other rib parameters used to roughened an air duct with a fixed value of Re=8000. It can be seen that the fluid temperature increases along the distance of the air duct, and the maximum fluid temperature is found at the outlet of the air duct. In general, it can be said that the augmentation of the heat transfer for different rib surfaces is produced by the increased turbulence. The supplementary augmentation might be due to the involvement of the secondary flow cells of the fluid along the ribs, which transmitted heated air away from the heated plate surface. It was found, out of all the V-rib combined with dimpled rib roughness shapes investigated, the flow attack angle of 55° had the highest fluid temperature (329 K) along the length of the air duct. This may be explained by the fact that shaping a long angled rib into a V-down shaped ribs combined with dimple ribs helps in the formation of two secondary flow cells and these secondary flow cells are responsible for increasing the fluid temperature along the length of the channel by separating the flow.

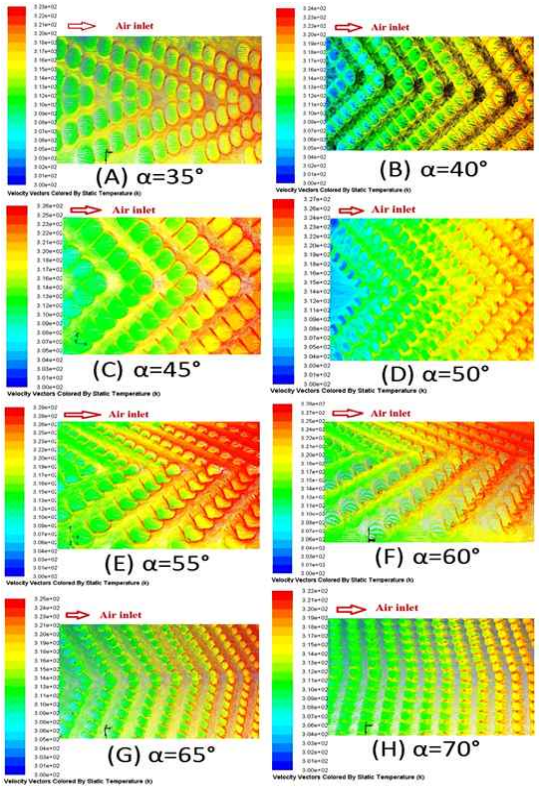

Fig. 4 Velocity vector .vs flow attack angle (Re=8000)

3.2 Heat transfer and fluid flow

The effect of flow attack angle and its location on an air duct heat transfer and fluid

flow characteristics was investigated for artificial roughened with V-pattern shaped ribs with compound dimple ribs. The heat transfer and fluid flow characteristics of the V-pattern shaped ribs combined with dimple ribs-roughened rectangular air duct were calculated on the basis of numerical data collected for various flow and roughness parameters. The present numerical results on heat and fluid flow characteristics in a uniform heat flux rectangular duct with the V-shaped ribs combined with dimple ribs are presented in the form of average Nusselt number ratios and average friction factor ratios. The average Nusselt number ratios obtained under turbulent flow conditions in all cases are presented in Fig.5. The average Nusselt number ratios increases with increase in Reynolds number as expected, due to increase in turbulent intensity with flow increase in Reynolds number, which leads to higher heat transfer. This is seen from Fig.5 that flow attack angle value of 55° yields the maximum heat transfer enhancement. This trends associated is due to the reason that the roughness interrupts the development of the boundary layer of the fluid flow and increase the degree of turbulence. For the roughness with α=55° shows a higher heat transfer rate and an enhancement of around 187%. The reason for average Nusselt number attaining a maximum value corresponding to the angle of attack value of 55° is separation of the secondary flow resulting from the presence of ribs and the movement of resulting vortices combining together to yield an optimum value of angle of attack.

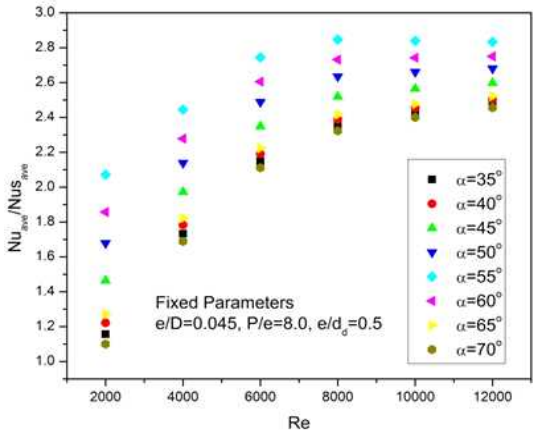

Fig. 5 Effect of flow attack angle on average Nusselt number ratios

Fig.6 shows the effect of path lines flow pattern on some selected flow attack angle values for Re=8000. It is seen that the maximum heat transfer performance in the present case has at the flow attack angle of 55°. As the flow attack angle is changed to a value below and higher 55°, the flow is not likely to reattach to the heat transferring surface before it reaches the successive rib. Therefore, the thermal performance of the duct deteriorates with decrease in the flow attack angle value below and higher 55°.

Enhancing the heat transfer by application of roughness will increase the average friction factor which boosts the pumping power requirements. The variation of average friction factor as a function of Reynolds number for different values of flow attack angle and fixed values of other roughness shape parameters has been shown in Fig.7.

Average friction factor increases with increase in angle of attack, attains a maximum value corresponding to angle of attack value of 55° and decreases with further increase in angle of attack value. The least and maximum value of friction factor have been obtained corresponding to angle of attack values of 70° and 55° respectively.

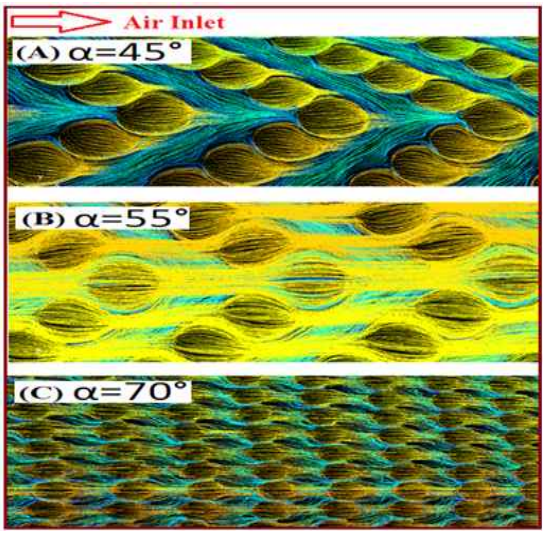

Fig. 6 Path lines for different flow attack angles (Re=8000)

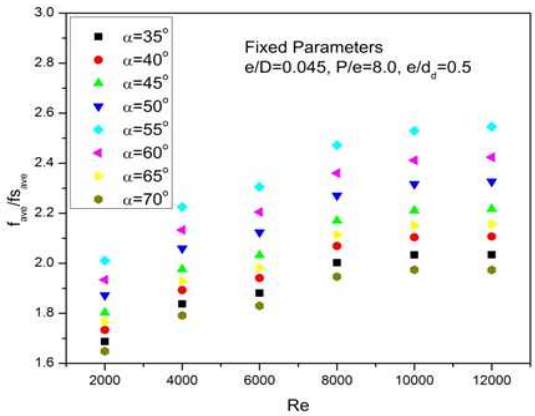

Fig. 7 Effect of angle of attack on average friction factor ratios

3.3 Overall thermal performance

The numerical results predicted an increase in average Nusselt number ratios (Nu_{ave}/Nus_{ave}) with increasing flow attack angle, however average friction factor ratios(f_{ave}/fs_{ave}) also increased. The air duct efficiency therefore depended on these two parameters. The air duct performance enhancement owing to the rib roughness is normally evaluated on the base of the overall performance parameter, which includes both the thermal and hydraulic concerns. The overall performance parameter was defined as the overall enhancement ratio and expressed as follows[31]:

$$\eta = (N_{ave}/Ns_{ave})(f_{ave}/fs_{ave})^{0.33} \quad (10)$$

It is apparent that only a heated surface roughness that yields a performance parameter value greater than unity is useful. The higher the value of this parameter, the better the solar air channel performance. Fig.8 shows the overall performance parameter for the air duct with different values of flow attack angle for range from 2000 to 12,000. It increased with increases in the flow attack angle up to about 55° and then decreased with further increases in the flow attack angle at all values. It therefore attained a maximum at a flow attack angle of about 55°. The values of thermo-hydraulic performance parameter determined for the shape of V-shaped ribs combined with dimple ribs have been compared with the values determined for dimple rib shape[23], V-down rib shape[20]

and V-down pattern rib shape.[22] Fig.9 shows the V-shaped ribs combined with dimple ribs shape results in best thermo-hydraulic performance among all the geometries investigated. The effect of V-shaped rib with combined dimple rib in SAH duct is studied by comparing the thermo-hydraulic performance results of present study with other rib shapes (V-shaped rib, V-down shaped rib and dimple rib) as presented in Fig.9 The V-shaped rib with combined dimple rib with flow attack angle of 55° was considered for comparison as it yielded best thermo-hydraulic performance. The rib height, rib pitch and angle of attack roughness parameters for other rib shapes (V-shaped rib, V-down shaped rib and dimple rib) were same. It has been clarified in some of the previous studies that the propagation of secondary fluid flow cells along the inclined rib is responsible for the higher order of turbulence and heat transfer in the inter-rib region. The secondary fluid flow undergoes a rise in temperature from leading to trailing end of the rib. Due to higher heat transfer performance of inclined rib, the V-shape rib roughness has been developed for further enhancement of convective heat transfer rates.

The compound roughness of V-shaped ribs and dimples considered here increases local Nusselt number through the dimples. It is noted that the higher heat transfer rate is attributed to the interaction of secondary flow through the dimple rib in V-pattern rib with in main flow. The high velocity secondary flow jet approaches the dimple rib with V-pattern rib and produces additional turbulence by separation and reattachment on the top and the two sides of it. The thermo-hydraulic performance of SAH duct roughened with V-shaped rib combined with dimple rib shows higher than that roughened with V-shaped rib, V-down shaped rib and dimple rib as shown in Fig.9

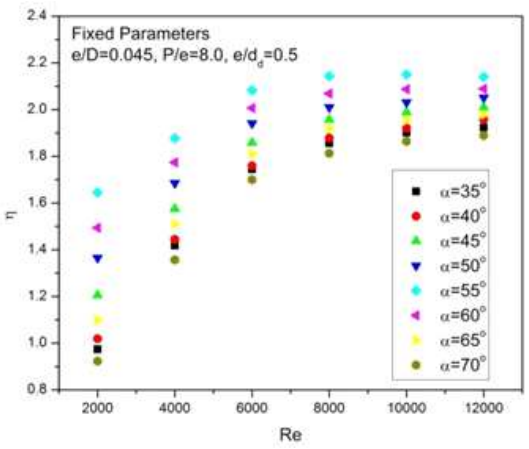

Fig. 8 Effect of angle of attack on overall thermal performance

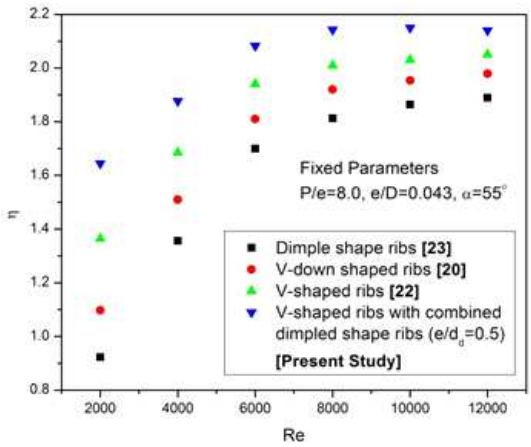

Fig. 9 Comparison of thermo-hydraulic performance with previous investigation

4. Conclusions

On the basis of critical analysis of results obtained from the CFD on SAH duct provided with V-pattern shaped ribs combined with dimple ribs yields the following conclusions drawn:

(1) CFD method is used in the present work for analyzing and optimizing the roughness under consideration. The RNG k-ε turbulent model predicted very close results to the experimental results, which yields confidence in the predictions done by numerical analysis in the present investigation.

(2) Both the average Nusselt number ratios and average friction factor ratios are strong function of flow attack angle. The highest average Nusselt number ratios and average friction factor ratios occur at the flow attack angle of 55°.

(3) The maximum value of thermo- hydraulic performance parameter is 2.18 corresponding to the flow attack angle of 55°. The value of thermo- hydraulic performance parameter for V-pattern shaped ribs combined with dimple ribs larger than that for dimple rib shape and V-pattern rib shape SAH duct.

Reference

1. A. Kumar, M.-H. Kim. Numerical optimization of solar air heaters having different types of roughness shapes on the heated plate - Technical note, Energy, Vol. 72, pp.731-738, 2014.
2. A. Kumar, R.P. Saini, J.S. Saini. A review of thermo-hydraulic performance of artificially roughened solar air heaters, Renewable and Sustainable Energy Review, Vol. 37, pp. 100-122, 2014.
3. A. Kumar, R.P. Saini, J.S. Saini. Heat and fluid flow characteristics of roughened solar air heater duct-A review, Renewable Energy, Vol. 47, pp. 77-94, 2012.
4. A. Kumar, R.P. Saini, J.S. Saini. Effect of roughness width ratio in discrete Multi v-shaped rib roughness on thermo-hydraulic performance of solar air heater, Heat and Mass Transfer, Vol. 51, pp. 209-220, 2015.
5. A. Pundir, A. Kumar, Technical feasibility study for power generation from a potential mini hydro site nearby Shoolini University, Advances Energy Research, Vol. 4, pp. 85-95, 2014.
6. A. Kumar. Analysis of heat transfer and fluid flow in different shaped roughness elements on the absorber plate solar air heater duct, Energy Procedia, Vol. 57, pp. 2102-2111, 2014.
7. J.C. Han, L.R. Glicksman, W.M. Rohsenow. An investigation of heat transfer and friction for rib-roughened surfaces. Int. J. of Heat and Mass Transfer, Vol. 21, pp. 1143 - 1156, 1978.
8. J.S. Park, J.C. Han, Y.Huang. Heat transfer performance comparisons of five different rectangular channels with parallel angled ribs. Int. J. of Heat and Mass Transfer, Vol. 35, pp. 2891 - 2903, 1992.
9. S.C. Lau, R.D. Mcmillin, J.C. Han. Turbulent heat transfer and friction in a square channel with discrete rib turbulators. Journal of Turbomachinery, Vol. 113, pp. 360 - 367, 1991.
10. Y.M. Zhang, W.Z. Gu, J.C. Han. Heat transfer and friction in rectangular channels with ribbed or ribbed-grooved walls. Journal of Heat Transfer, Vol. 116, pp. 58 - 65, 1994.

11. K. Prasad, S.C. Mullick. Heat transfer characteristics of a solar air heater used for drying purposes. Applied Energy, Vol. 13, pp. 83 - 93, 1983.
12. B.N. Prasad, J.S. Saini, Effect of artificial roughness on heat transfer and friction factor in a solar air heater. Solar Energy, Vol. 41, pp. 555-560, 1988.
13. M.M. Sahu, J.L. Bhagoria, Augmentation of heat transfer coefficient by using 90° broken transverse ribs on absorber plate of Solar air heater, Renewable Energy, Vol. 30, pp. 2075-2063, 2005.
14. R. Kiml, S. Mochizuki, A. Murata, Effects of rib arrangements on heat transfer and flow behaviour in a rectangular rib roughened passage Journal of Heat Transfer, Vol. 123, pp. 675-681, 2001.
15. D. Gupta, S.C. Solanki, J.S. Saini, Thermohydraulic performance of solar air heaters with roughened absorber plates, Solar Energy, Vol. 61, pp. 33 - 42, 1997.
16. H.H. Cho, Y.Y. Kim, D.H. Rhee, S.Y. Lee, S.J. Wu. The effect of gap position in discrete ribs on local heat/mass transfer in a square duct, Journal of Enhanced Heat Transfer, Vol. 10, pp. 287-300, 2003.
17. K.R. Aharwal, B.K. Gandhi, J.S. Saini, Experimental investigation on heat-transfer enhancement due to a gap in an inclined continuous rib arrangement in a rectangular duct of solar air heater, Renewable Energy, Vol. 33, pp. 585 - 596, 2008.
18. J.C. Han, Y.M. Zhang, C.P. Lee, Influence of surface heat flux ratio on heat transfer augmentation in square channels with parallel, crossed and v-shaped angled ribs. Journal of Turbomachinery, Vol. 114, pp. 872-880, 1992.
19. R.T. Kukreja, S.C. Lau, R.D. McMillin, Local Heat/Mass transfer distribution in a square channel with full and V-shaped ribs. Int. J. of Heat and Mass Transfer, Vol. 36, pp. 2013-2020, 1993.
20. M.E. Taslim, T. Li. D.M. Krecher, Experimental heat transfer and friction in channel roughened with angled, v-shaped and discrete ribs on two opposite walls, Journal of Turbomachinery, Vol. 118, pp. 20-28, 1996.
21. L.M. Wright, W.L. Fu, J.C. Han, Thermal performance of angled, V-shaped and W-shaped rib turbulators in rotating rectangular cooling channels (AR=4:1), Journal of Turbomachinery, Vol. 126, pp. 604 - 614, 2004.
22. A.M.E. Momin, J.S. Saini, S.C. Solanki, Heat transfer and friction in solar air heater duct with v-shaped rib roughness on absorber plate. In.t. J of Heat and Mass Transfer, Vol. 45, pp. 3383 - 3396. 2002.
23. R.P. Saini, J. Verma, Heat transfer and friction factor correlations for a duct having dimple-shaped artificial roughness for solar air heaters. Energy, Vol. 133, pp. 1277 - 1287, 2008.
24. A. Chaube, P.K. Sahoo, S.C. Solanki. Analysis of heat transfer augmentation and flow characteristics of a solar air heater. Renewable Energy, Vol. 31, pp. 317 - 331, 2006.
25. S. Kumar, R.P. Saini. CFD based performance analysis of a solar air heater duct provided with artificial roughness, Renewable Energy, Vol. 34, pp. 1285-1291, 2009.
26. R. Mehrdad, R. Arman, Prediction of turbulent flow and heat transfer in channels with array of detached and alternative attached-detached ribs, Int. J. of Numerical Methods for Heat & Fluid Flow, Vol. 19, pp. 266-284, 2009.
27. S.V. Karmare, A.N. Tikekar. Analysis of fluid flow and heat transfer in a grit roughened surface solar air heater using CFD. Solar Energy, Vol. 84, pp. 409-417, 2010.

28. M. Oronzio, N. Sergio, R. Daniele. Numerical investigation of air forced convection in channels with differently shaped transverse ribs, Int. J. of Numerical Methods for Heat & Fluid Flow, Vol. 21, pp. 618-639, 2011.
29. A.K. Sharma, N.S. Thakur. CFD based fluid flow and heat transfer analysis of a v-shaped roughened surface solar air heater. Int. J. of Engineering Science and Technology, Vol. 4, pp. 2115-2121, 2012.
30. A. S. Yadav, J.L. Bhagoria, A numerical investigation of square sectioned transverse rib roughened solar air heater, Int. J. of Thermal Sciences, Vol. 79, pp. 111-131, 2014.
31. M.J. Lewis. Optimizing the thermo-hydraulic performance of rough surfaces. Int. J. of Heat and Mass Transfer, Vol. 18, pp. 1243 - 1248, 1975.